Ermina Begovic
Carlo Bertorello
Simone Mancini

ISSN 0007-215X
eISSN 1845-5859

HYDRODYNAMIC PERFORMANCES OF SMALL SIZE SWATH CRAFT

UDC 629.5.52:629.5.022.25:629.5.015.2
Original scientific paper

Summary

The good seakeeping characteristics of SWATH hull form are very interesting for small working craft and pleasure boats. Intrinsic limitations as the low values of weight per inch of immersion and transversal and longitudinal instability, can be acceptable and successfully managed when the mission profile does not ask for significant load variation and shift. The exploitation of SWATH concept is limited by the craft size, but if main dimensions allow enough static stability, this configuration appears very promising. SWATH behaviour in rough sea at zero and low speed have led to consider this hull form within the small craft design research program in progress at University of Naples Federico II.

The design of small size SWATH working/pleasure craft has to begin from the consideration of strut waterplane areas that are the key factor to get acceptable static and dynamic stability. Displacement has to be reduced as most as possible to increase static stability, as shown by last design trends. The results of CFD analysis concerning SWATH resistance and propulsion, aspects are presented. A numerical evaluation of the hull-propeller interactions is performed, through simulations of self-propulsion tests with a simplified method (Actuator Disk model) to discretize the propeller effect. The effective wake coefficient, the thrust deduction fraction and hull efficiency are provided. To validate CFD resistance results a comparison with experimental tests performed by Authors is reported.

The presented work highlights different hydrodynamic aspects, comments advantages and critical issues of SWATH concept and reports detailed CFD modelling procedure with the aim to provide a reference for SWATH small craft design.

Key words: *SWATH hull form design; SWATH dynamic instability; SWATH CFD resistance assessment; numerical self-propulsion test; propulsion coefficients;*

1. Introduction

The growing activities for offshore wind farms maintenance and survey, as well as the interest about small suppliers for coastal oil platforms, focused small craft designer attention about the lowest possible wave responses at zero or very low speed. The ability to be moored or to stay close to a fixed body with the smallest possible vertical motions is very important for the successful design of small craft operating at open sea. Reduced vertical motions are considered a design criteria and represent the main limit for the ship operability.

Although SWATH craft presents very good seakeeping characteristics, when main dimensions are small, the low values of unit displacement and of transversal and longitudinal stability limit a sound application of such hull form.

The idea of SWATH derives from semi-submersible offshore rigs, which are designed to provide a working platform with minimized motions in open sea. The buoyancy of a SWATH ship is mainly provided by its submerged torpedo-like bodies, which are connected by single or twin struts to the upper platform. The waterplane is minimised to reduce the vertical loads induced by waves. The vertical motions are quite smaller in comparison to catamarans and monohulls of similar displacement, although SWATH behaviour has to be carefully studied to avoid resonance in working conditions.

Beside these very interesting characteristics, SWATHs pose some problems. They are very sensitive to weight distribution and dynamically instable when relative speed increases. As regards motion resistance their performances are in the same range of conventional hull forms, except at very low relative speeds when larger wet surface worsen their performances. In following sea, the pitch response is of particular concern because very large encounter periods, close to the pitch resonance, are likely to occur over a wide range of wave lengths.

SWATH concept has been considered for more than forty years and several modifications of the original basic concept have been performed. At present, the four struts configuration appears preferable versus the twin one and it is used for the small size craft considered in this paper. The reason lies in better longitudinal stability due to the optimal longitudinal distribution of strut waterplane areas.

Strut waterplanes can have different shapes, in any case very slender. A very effective and commonly chosen shape has parabolic sides, symmetrical in respect to both strut centre line and mid length. Torpedos are very slender bodies and can be simplified to get simple and cheap construction. Generally, they present an hemispheric bow, a cylindrical part and a conic tail, as shown in Figure 1. There is plenty of research about such bodies totally immersed in a fluid. Streamlined longitudinal profiles are generally superior in terms of resistance; some designs have considered these more complicated shapes when dealing with resistance optimisation for higher speed. Basic circular sections have been modified in some cases when an optional catamaran cruising condition is considered. Anyway, the above general considerations have to be revised to fit the SWATH vessel peculiar characteristics and mission profile.

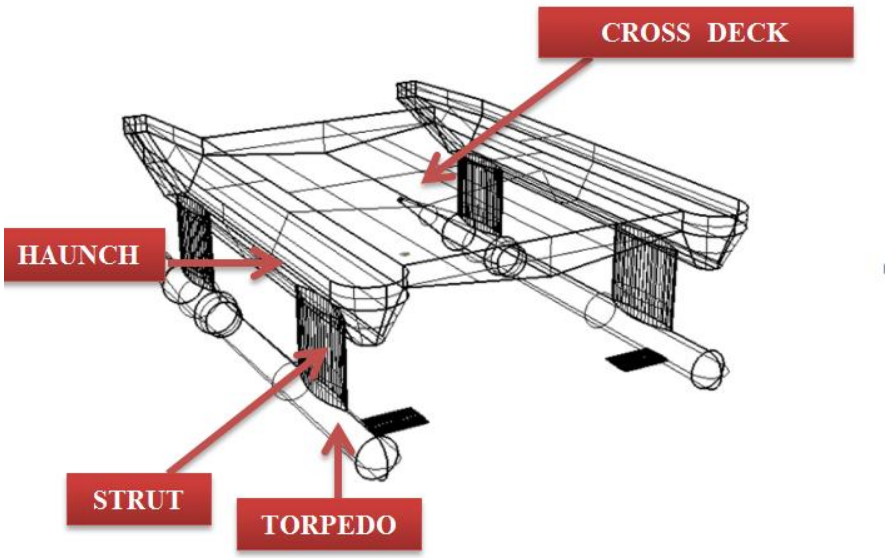

Fig. 1 SWATH hull components

Since the milestone work of Lee and Curphey [1] it has been pointed out that:

- SWATH ships are dynamically unstable and there is a necessity of fins to maintain heave and pitch stability at high speeds;
- peak motions in heave, roll and pitch are excited in longer waves;
- wave exciting heave force and pitch moment acting on SWATH are smaller than those acting on a monohull of comparable displacement.

Salvesen et al [2] developed a numerical method for wave resistance optimization of torpedo hulls valid for any cross section shape, not only bodies of revolution. Furthermore, authors considered struts shape as a constrain and wave minimization is obtained by reshaping the torpedo hulls. Papanikolau et al [3] applied optimization procedure based on Salvesen [2] method for SWATH in the range of Froude numbers from 0.3 to 0.7. According to the service speed, the displacement of torpedo tends to be concentrated around the midship section (for low Fr) or towards the ends (for high Fr). For this optimized SWATH, Schellin et al [4] reported seakeeping predictions compared against experimental data indicating good overall performances but also necessity of stabilizing fins. Beena et al [5] presented seakeeping analysis of different torpedo forms, and discussion on the appropriate criteria for pitch, roll and vertical accelerations. Authors suggested that higher amplitudes may be imposed in the range of frequencies typical for SWATH motions, identifying a limiting value of 8 degree for roll and 0.4g for vertical acceleration and 3 degree for pitch RMS. Yoshida [6] introduced "resonance free SWATH" obtained by diminution of strut length to approximately one half of torpedo length. Brizzolara et al [7, 8] presented an example of the so called "2nd generation SWATH". Authors reported that for Fr>0.5, the position of contracted section remains almost invariably at midship, independently from the prismatic coefficient C_P, the slenderness coefficient $L/V^{1/3}$ or the ratio L/D. As maximum weight and dimensions were the assigned design constraints, the strut length decreased drastically, and to obtain the sufficient initial transversal and longitudinal metacentric height, four struts were chosen and positioned at the extreme bow and stern of the torpedo hull. Qian et al [9] investigated a SWATH vehicle with inclined struts by numerical and experimental methods reporting that the inclined struts performed better seakeeping performances in comparison with a vertical-strut SWATH. Begovic and Bertorello [10] presented SWATH yacht design reporting extensive resistance and seakeeping experimental results performed at University of Naples Federico II.

The present paper reports a numerical approach of hydrodynamic assessment of SWATH concept. Numerical simulations in *CD Adapco StarCCM +* are performed for four model speeds. The paper reports complete procedure and comparison with experimental data obtained by Authors and presented in previous work [9]. For the considered speeds, the simulations of self-propulsion tests have been performed and the results are elaborated in terms of thrust deduction, wake and hull efficiency coefficients.

Dynamic instability of SWATH craft at higher speeds, resulting in excessive dynamic trim, is counteracted in service by active stabilizing fins. In the CFD simulations, three different setups have been considered: hull restrained for trim only, restrained for sinkage and trim, free for sinkage and trim. Experimental tests have been performed with trim restrain acting as soon as the minimum trim angle has been recorded. This in order to appreciate the maximum possible free ride speed and then to consider the action of trim correctors. Experimental setup is very close to restrained model numerical simulation set up.

The present work highlights different hydrodynamic aspects, commenting advantages and critical issues of SWATH concept, reports detailed CFD procedure for resistance and propulsion test simulation, and can be used as a reference for SWATH small craft design.

2. DESIGN of SWATH small size pleasure/working craft

Several developments of the SWATH concept have been tried since the first applications in the late sixties. Although the expected seakeeping performances are related to smallest possible waterplanes, it must be considered that SWATH vessels, as any floating body follow Euler's law for ship stability. This means that both waterplane area, through second order moment, and hull volume, that is to say ship weight, affect metacentric radius. This aspect has to be considered at preliminary design stage taking into account both factors as well as a realistic CG vertical position.

Generally, static stability is not problematic for larger SWATH vessels but it becomes a design criteria for smaller craft and represents the lowest limit to main dimensions for a practical application of the concept. The use of composites in some of the most recent small size constructions could be surprising at first sight, but witnesses the importance of the reduction of structural weight and displaced volume related to stability issues. Within design development, the general used procedure to check the (transversal) stability of a given hull form according to defined criteria, could lead to significant loss of design time. For SWATHs it is preferable to identify the maximum allowable heeling angles (both longitudinal and transversal) for a given heeling moment coherent with mission profile and ship characteristics.

The scale model considered in this paper is relative to a SWATH 32 m L_{OA} motor yacht. For this ship, a value of 2 degrees maximum longitudinal or transversal inclination due to 6 crew and 12 passengers crowding on one side has been assumed. This value is quite lower than the maximum of 10 degrees allowed by Classification Societies (RINA, Rules for Pleasure Yachts 2013, Ch.6, Par. 2 /2.1/2.1.1/g).

Then the waterplane area second order moment can be calculated, and stability evaluated for Displacement and VCG based on reliable data. The second order moment is divided into two or four contributes according to the chosen number of struts and the single strut waterplane can be drawn. This last has parabolic sides and cord/camber ratio not lower than six, if service speed leads to a significant wave resistance component. In case of very slow vessels, larger and squatter waterplane can be accepted. With this procedure, the strut waterplane area is set to the minimum possible value and SWATH concept used at its best.

From these considerations it is evident that it is very difficult to use SWATH concept for small craft. In practice, there is no manned SWATH vessel below 12 m L_{OA}.

The present design trend features four struts and twin torpedoes configuration. Above the struts a catamaran demi-hull with trapezoidal transversal sections assures buoyancy and stability when longitudinal and/or transversal heeling angles reach dangerous values. This configuration reported in the following Figure 2 appears the most promising to exploit SWATH peculiar characteristics in terms of reduced wake and motions with adequate safety margins provided by the upper catamaran hulls. Strut height is a compromise between the highest encounter wave height and maximum allowable draft. A V shaped cross deck bottom can add useful damping in case of impact with the sea surface. This configuration can be defined through few significant parameters as reported in the following Table 1. SWATH reported in Fig. 2 is relative to a pleasure/small working craft 1/32 scale model developed at the University of Naples Federico II.

Table 1 Principal parameters of SWATH configuration

	PARAMETER	SI Unit	MODEL	SHIP
TORPEDO	*L_T*	(m)	0.970	31.04
	Radii	(m)	0.030	0.960
	Head	(m)	0.030	0.960
	Tail_Length	(m)	0.197	6.304
	Tail_End Radius	(m)	0.005	0.160
	Wetted Surface	(m^2)	0.167	171.295
STRUT	*No*	-	4	4
	Length L_S	(m)	0.150	4.800
	Camber	(m)	0.026	0.832
	C_{WP}	-	0.680	0.680
	Wetted Surface	(m^2)	0.01965	20.122
SWATH	*Displacement*	(kg, t)	5.6	188.088
	Beam over all	(m)	0.600	19.200
	Beam @ strut CL	(m)	0.540	17.280
	Immersion	(m)	0.125	4.016
	Wetted Surface	(m^2)	0.41316	423.076
	D_T/T	-	0.48	0.48

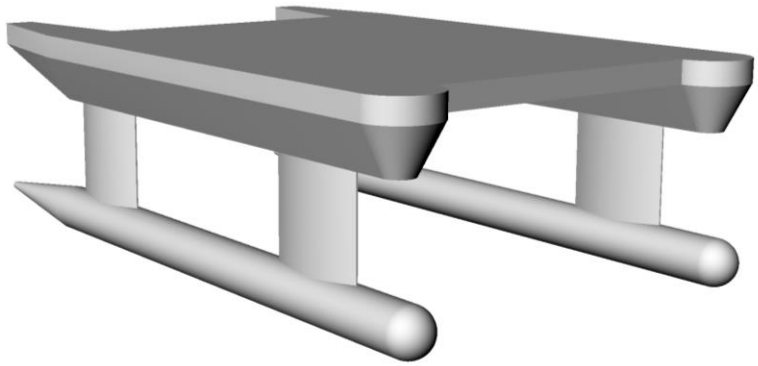

Fig. 2 Designed SWATH hull

The parameters with intrinsic limitations are:

- strut camber, to allow access to the engine inside torpedo;
- torpedo diameter, to provide enough room for engine housing;
- minimum waterplane area, to allow positive metacentric height at rest.

These considerations are valid in the most common case of diesel propulsion with each engine housed into one torpedo and the obvious need to access it for control and maintenance without dry dock the ship. In case of different system layouts or if dry dock is considered for any type of engine maintenance (as in case of full electric propulsion) the previous considerations can be forgotten and the strut camber can be optimized and limited only by stability.

2.1 Dynamic Stability

When dynamic forces and moments became of the same order of hydrostatic ones SWATH configuration became intrinsically unstable. Longitudinal instability is much more evident as longitudinal position of centre of hydrodynamic forces shifts according to speed variation and the longitudinal equilibrium with the weight forces applied in the *LCG* is modified resulting in large trim changes. In case of very small strut waterplane areas, a stable trim at rest does not assure stability at speed as in standard displacement vessels and becomes necessary to consider the involved factors to identify adequate countermeasures.

Although torpedoes are generally axial symmetrical bodies, the pressure field around them it is not. They are not deeply immersed and the pressure field around them is influenced by the free surface. This phenomenon is well known as surface suction in submarine hydrodynamics, when such vessels travel close to the free surface, Renilson [11, 12, 13], Bhattacharyya [14].

At speed, the forward strut wave system further modifies the free surface and the pressure field around the torpedo. In calm water, the surface suction is due to the Venturi effect, which results in higher flow velocity between torpedo and free surface and therefore lower pressure. This causes a pitch moment, variable with torpedo's forward speed and with immersion.

Struts resistance has different contribution in respect to the torpedoes one as speed increases. At lowest speed there is almost no wave system around the strut in an almost total viscous and viscous pressure resistance regime; the wetted surface is the key parameter and the struts have quite less influence in respect to torpedoes. Increasing relative speed the struts, resistance is increased significantly by wave component. This factor enhances the shifting upward of resistance point of application and can explain the observed stern down trim at speed.

Nevertheless, SWATH longitudinal instability cannot be so easily simplified. Even if a small pitch angle is given to torpedoes, they act as foil and tend to increase the angle as speed increases. The strut unitary displacement is too low to counteract such effect and the hull can change trim stern or bow down according to the initial trim perturbation. The trim change can be stopped only by larger volume reaching the water with large resistance increase or by sudden intervention of trim correctors.

After these considerations, it is evident that a full exploitation of the SWATH concept is possible only through an effective stabilizing device which action must be more powerful as speed increases. Transversal dynamic stability is generally larger and adequate at any speed.

3. NUMERICAL ASSESSMENT OF SWATH HYDRODYNAMIC PROPERTIES

Numerical simulations in *CD Adapco Star-CCM+* v9.06 *RANS* software have been performed for four model speeds: 0.976, 1.301, 1.952, 2.603 m/s corresponding to Fr_T = 0.316, 0.422, 0.633 and 0.844. For the considered model-ship scale λ = 32, these velocities correspond to full scale speed of 10.73, 17.89, 21.47 and 28.62 kn, i.e. speed range reasonable for small size craft service. The SWATH intrinsic instability, required a non conventional approach for the numerical simulation of resistance test using the Chimera grid, also called overset grid technique. In particular this approach permit to not loose numerical accuracy in inclined positions. The unstructured mesh with the fixed and moving regions, shown in Fig. 3, is used for the computations. The grid sensitivity analysis has been performed for resistance test at model speed of 0.976 m/s for three different grids, reported in details in Section 3.4. The chosen mesh, i.e. number of cells and base sizes for both tank (fixed) and overset regions are given in Table 2.

Table 2 Mesh properties summary

Type of mesh	Trimmed/ polyhedral
No. of cells – tank	358468
Base size - tank (m)	2.3
No. of cells – overset	1210190
Base size – overset (m)	0.65

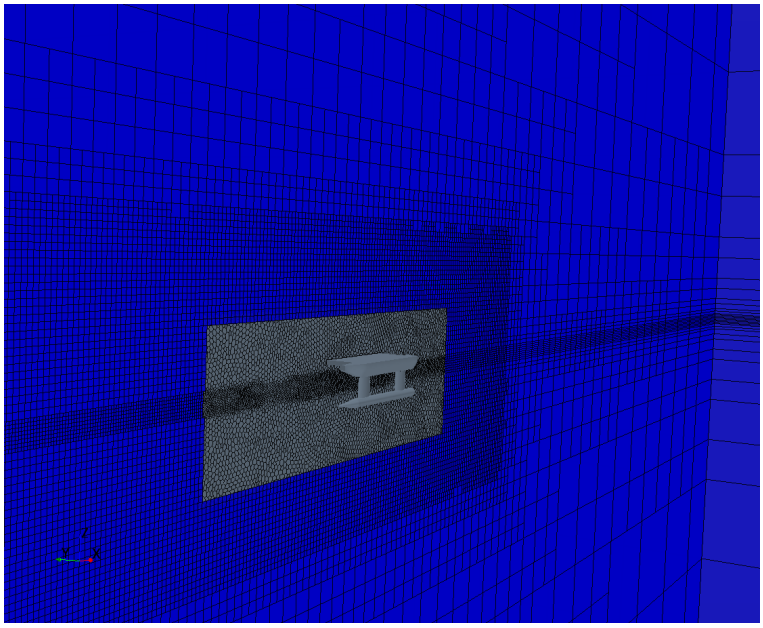

Fig. 3a Numerical set up- Mesh used and different regions visualization: fixed - blue and overset - gray

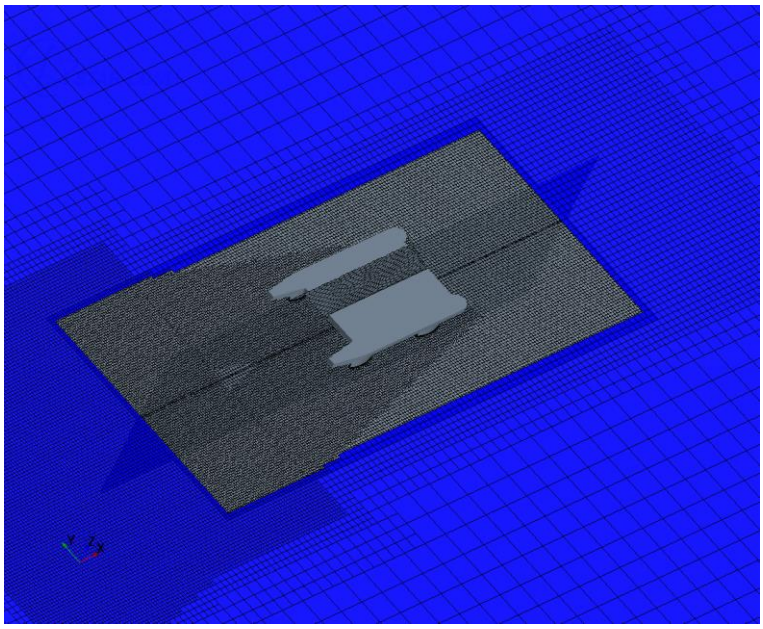

Fig. 3b Numerical set up- Mesh used and different regions visualization: fixed - blue and overset - gray

3.1 Numerical set up

To solve the time-marching equations, an implicit solver is used to find the field of all hydrodynamic unknown quantities, in conjunction with an iterative solver to solve each time step. The software uses a *Semi Implicit Method for Pressure Linked Equations* to conjugate pressure field and velocity field, and an *Algebraic Multi-Grid* solver to accelerate the convergence of the solution. The free surface is modelled with the two phase volume of fluid technique (*VoF*). A segregated flow solver approach is used for all simulations.

Coordinate system origin has been imposed in centre of buoyancy of torpedo hull.

The Reynolds stress problem is solved by means of K-Omega SST turbulence model and the All Wall y+ is the wall treatment utilized for all simulations. It is a hybrid approach that attempts to emulate the high y+ wall treatment for coarse meshes (for y+ > 30), and the low y+ wall treatment for fine meshes (for y+ ≈ 1). It is also formulated with the desirable characteristic of producing reasonable answers for meshes of intermediate resolution (for y+ in the buffer layer), *CD Adapco Star-CCM+* v9.06 User's Guide [20]. This approach is considered a reasonable compromise among the acceptable quality of the boundary layer description and the calculation time. The y+ variation on the strut and torpedo is given in Fig. 4a-d for the four velocities examined. It can be seen that y+ values range from 0 to 25.

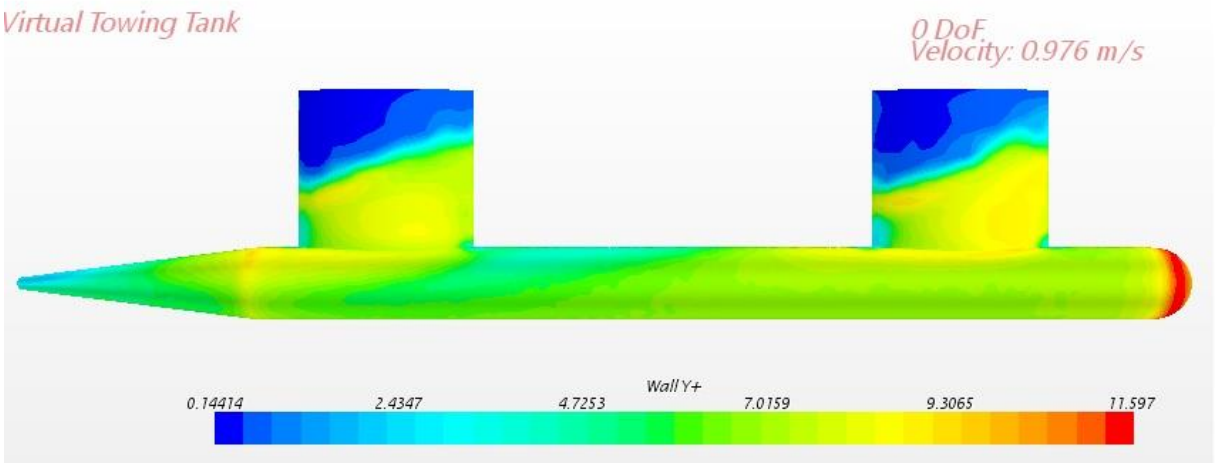

Fig. 4a y+ values in 0DOF simulation at model speed 0.976 m/s

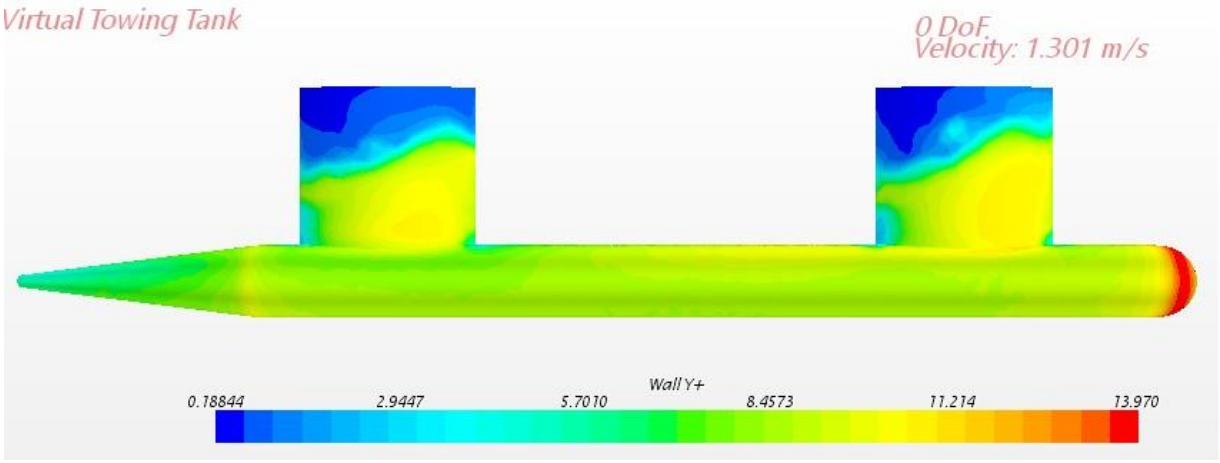

Fig. 4b y+ values in 0DOF simulation at model speed 1.301 m/s

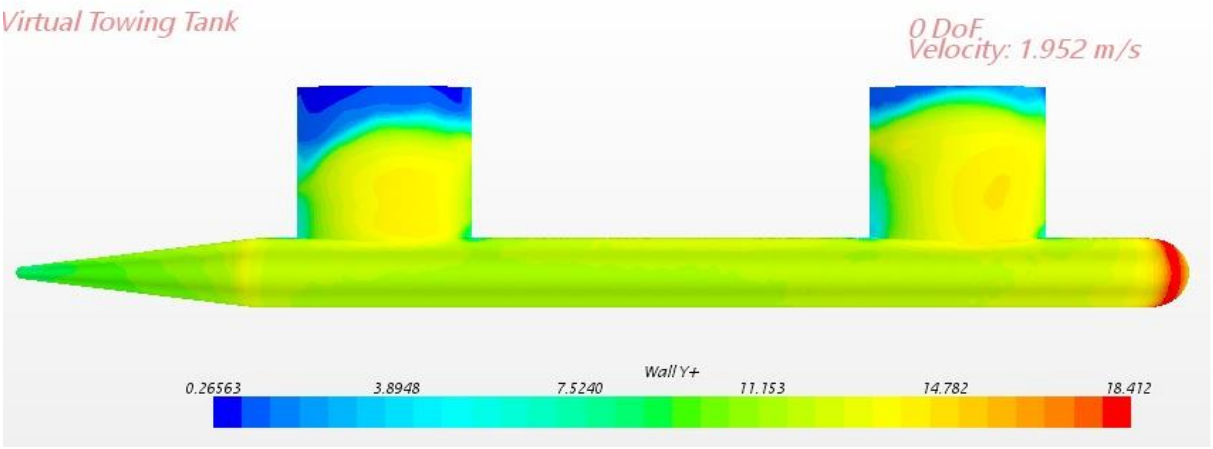

Fig. 4c y+ values in 0DOF simulation at model speed 1.952 m/s

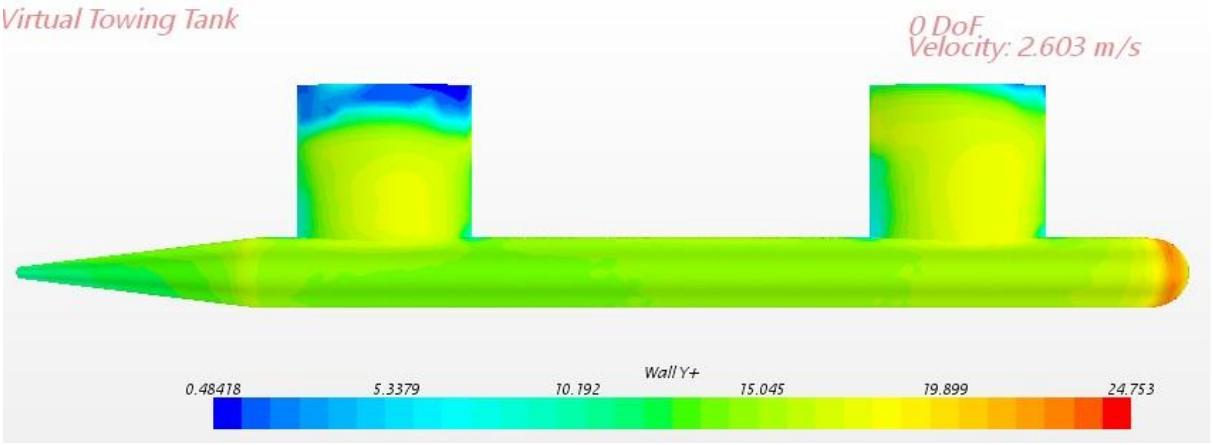

Fig. 4d y+ values in 0DOF simulation at model speed 2.601 m/s

All properties of the numerical solver are reported in Table 3. Boundary conditions are illustrated in Fig. 5 and listed in Table 4.

Table 3 Numerical simulation set up summary

Pressure link	SIMPLE
Pressure	Standard
Convection Term	2nd Order
Temporal Discretization	1st Order
Time-step (s)	0.015
Iteration per t.s.	5
Turbulence Model	K-Omega SST

Table 4 Boundary conditions set up summary

Inlet	Velocity inlet condition
Outlet	Pressure outlet condition
Bottom/Top	Velocity inlet condition
Side	Symmetry condition
Hull	Wall with no-slip condition
Symmetry plane	Along centreline of the hull

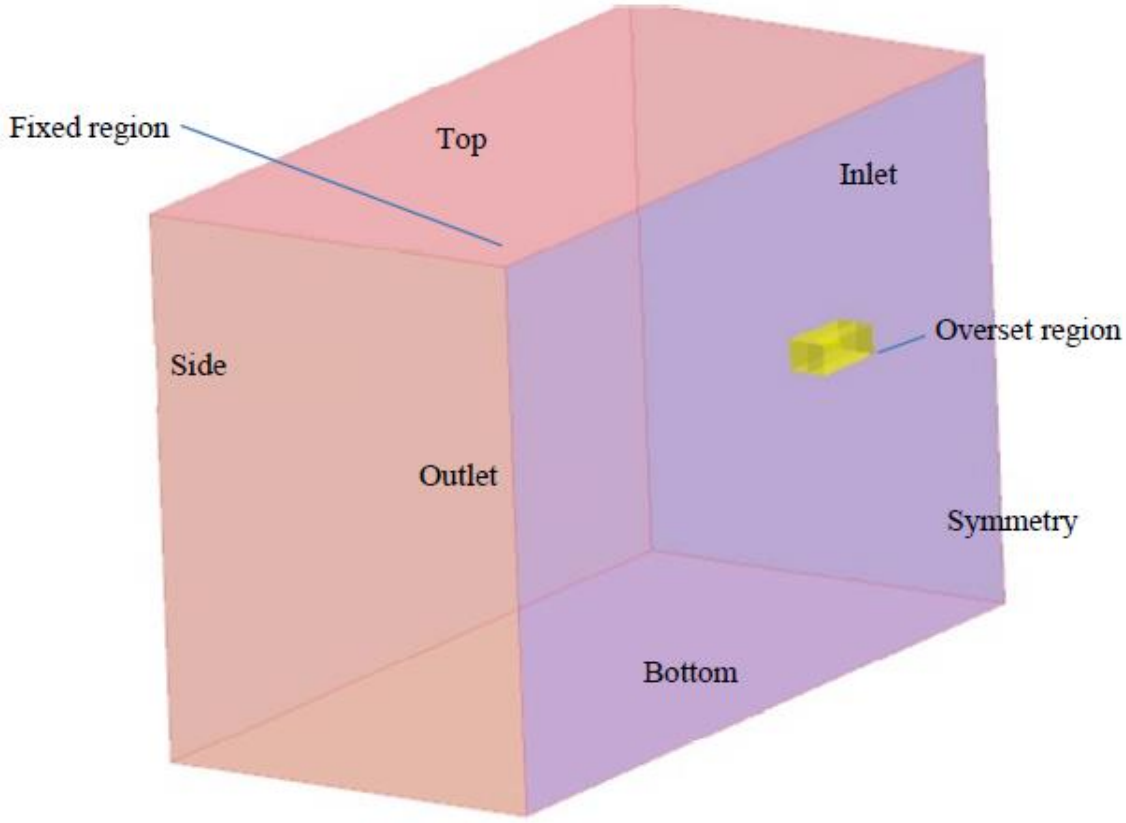

Fig. 5 Boundaries set up

All calculations have been performed at Calculation Centre of University of Naples Federico II, using 32 processors. For 30 seconds of physical time of resistance simulations, calculation time was about 30 hours.

3.2 Bare hull calm water resistance

Dynamic instability of SWATH craft at higher speeds, resulting in excessive dynamic trim, can be effectively counteracted in service by active stabilizing fins and in some cases by water ballast shifting. To get the whole picture of the possible running conditions, in the CFD simulations three different setups have been considered: hull restrained for trim only, restrained for sinkage and trim, free for sinkage and trim (2DoF). Simulations are performed for model speeds: 0.976, 1.301, 1.952 and 2.603 m/s. All CFD calculations are performed in model scale to compare easily and immediately numerical and experimental results. In coherence the grid sensitivity study was done at model scale. The aims of the paper are to validate CFD as design tool for swath configuration and to explore and identify speed limits for pure SWATH hullforms.

In the simulation with model free to heave and pitch (2DOF), the SWATH dynamic instability is observed at tested speed 1.952 m/s and 2.603 m/s. The result is aft down trim unless the catamaran hulls touch the water and provide restoring moment, as shown in Fig. 6 (lower).

In the second set of simulations (model restrained for pitch, and free only to heave), at higher speed (v = 1.952 and 2.603 m/s), the pitch constrain results in a downward force leading to strut further immersion as can be observed in Fig. 7 (lower). Finally, simulations for model restrained to heave and pitch have been performed and these results are illustrated in Fig.8. In all simulations SWATH initial trim is zero degree.

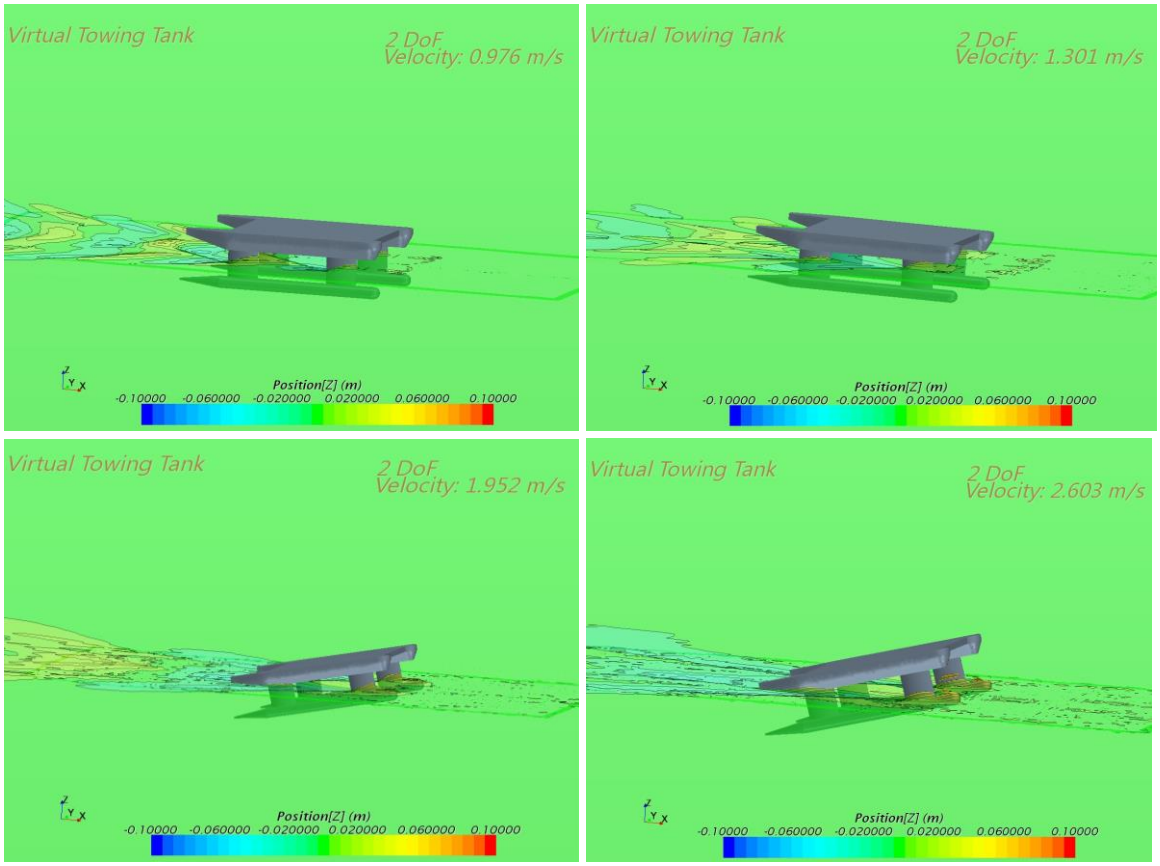

Fig. 6 SWATH resistance simulation results with model free for heave and pitch

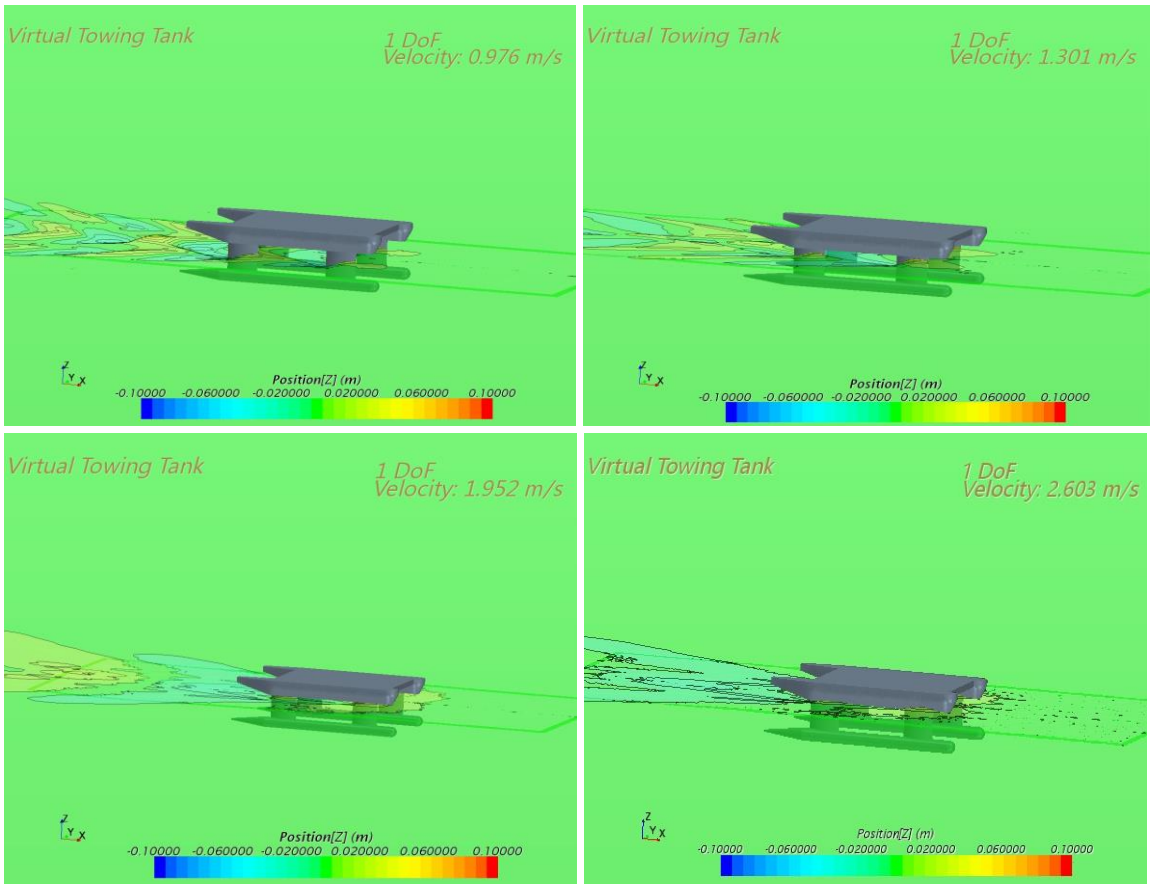

Fig. 7 SWATH resistance simulation results with model free to heave

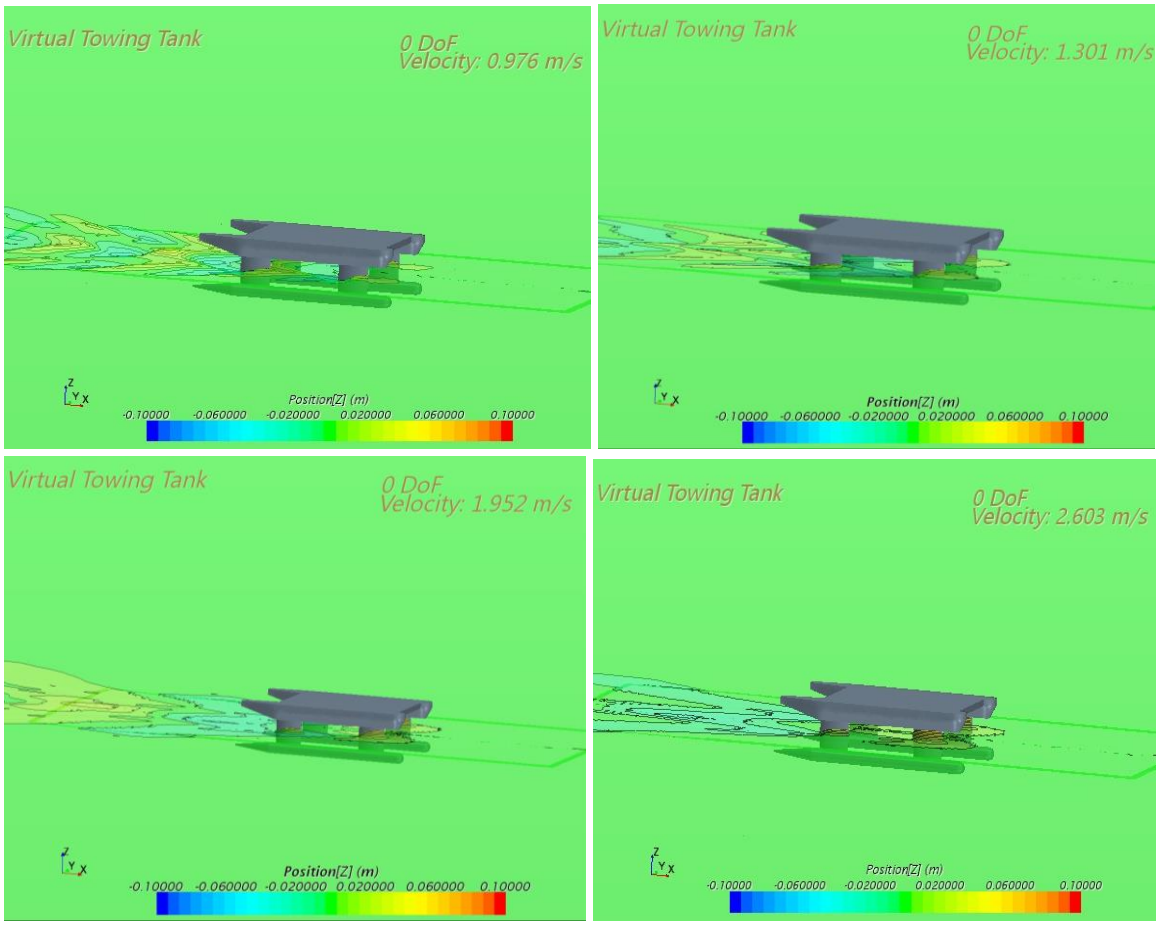

Fig. 8 SWATH resistance simulation results with model restrained for heave and pitch

Numerical results for total resistance, frictional resistance, trim, sinkage and wetted surface are summarised in Table 5, while in Fig. 9 wave making and frictional resistance coefficients curves for different simulation setups are shown.

Table 5 Numerical results summary

2 DOF					
v_{model}	$R_{T\text{-}SWATH}$	$R_{F\text{-}SWATH}$	*Trim*	*Sinkage*	*WS*
(m/s)	(N)	(N)	(deg)	(m)	(m^2)
0.976	3.046	1.184	-0.500	-0.017	0.412
1.301	3.614	2.004	1.300	-0.025	0.434
1.952	8.77	4.506	-12.930	-0.004	0.450
2.603	12.984	6.906	-15.350	0.001	0.444

1 DOF					
v_{model}	$R_{T\text{-}SWATH}$	$R_{F\text{-}SWATH}$	*Trim*	*Sinkage*	*WS*
(m/s)	(N)	(N)	(deg)	(m)	(m^2)
0.976	3.064	1.184	0.000	-0.017	0.412
1.301	3.572	1.97	0.000	-0.023	0.424
1.952	7.402	4.292	0.000	-0.046	0.482
2.603	12.644	7.368	0.000	-0.059	0.496

0 DOF					
v_{model}	$R_{T\text{-}SWATH}$	$R_{F\text{-}SWATH}$	*Trim*	*Sinkage*	*WS*
(m/s)	(N)	(N)	(deg)	(m)	(m^2)
0.976	2.748	1.11	0.000	0.000	0.392
1.301	3.132	1.816	0.000	0.000	0.398
1.952	5.918	3.728	0.000	0.000	0.426
2.603	9.4	6.174	0.000	0.000	0.446

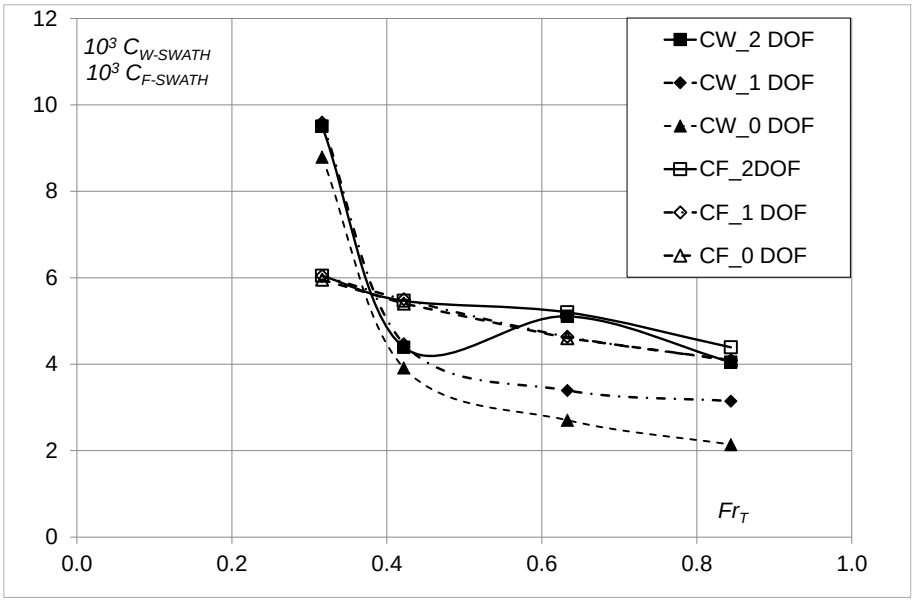

Fig. 9 Wave making and frictional resistance coefficients curves for different simulation setups

From resistance coefficients curves, shown in Fig. 9, it can be observed the effect of trim and sinkage on resistance performances. At first two speeds, the differences in frictional resistance coefficients are minimal as the waterplane area is almost identical for small variation of trim. There is no significant changing in wave pattern and in wetted surface among different simulations. This also means that the possible ide without constrain or stabilization for this SWATH configuration is up to Froude number Fr_T 0.422. At two higher speeds, trim angles obtained in simulation 2DOF are about 13 and 15 degrees, the wetted surface is about 15% higher than the one at rest and difference in total resistance between 2 DOF and 0 DOF is about 30%. As it can be observed in Fig. 9, the frictional resistance coefficient is slightly higher and the wave making resistance coefficient has been almost doubled with respect to 0 DOF.

The obtained results and moreover the sensibility of results with respect to degrees of freedom allowed in simulation are very important as it confirms the capacity of numerical method to predict reliable results. Further achievement is the possibility are to use the results from 2DOF and 1DOF simulation as input for trim corrector design, knowing exactly the trimming moment or the downward force to counteract. Furthermore, images and results also indicates that optimizing torpedo hull for wave resistance by potential flow solvers without considering free surface effects would lead to unrealistic conclusions for SWATH design and service capabilities.

3.3 Self-propulsion test simulations

The simulation of the propeller action and the individuation of the "self propelled point" has been performed using a uniform volume force distribution over a cylindrical disk having the same position and diameter of the propeller, called "Virtual Disk Model" (*VD).* The volume force varies in radial direction and the distribution of the force components, according to Visonneau et al [15] and Bugalski [16] is given by:

$$f_{bx} = A_x \cdot r' \cdot \sqrt{1 - r'} \tag{1}$$

$$f_{b\theta} = A_\theta \cdot \frac{r' \cdot \sqrt{1 - r'}}{r' \cdot (1 - r_h') + r_h'} \tag{2}$$

$$r_h' = \frac{R_H}{R_P} \qquad r' = \frac{r}{R_P} \tag{3}$$

where f_{bx} is the body force component in axial direction, $f_{b\theta}$ is the body force component in tangential direction, r is the radial coordinate, R_H is the hub radius and R_P the propeller tip radius. The constants A_x and A_θ are computed as

$$A_x = \frac{105}{8} \cdot \frac{T}{\pi \cdot d \cdot (3R_H + 4R_P) \cdot (R_P - R_H)} \tag{4}$$

and

$$A_\theta = \frac{105}{8} \cdot \frac{Q}{\pi \cdot d \cdot R_P \cdot (3R_H + 4R_P) \cdot (R_P - R_H)} \tag{5}$$

where d is the propeller thickness and T and Q are thrust and torque respectively. The computation of the body force components necessitates several user inputs. A propeller performance curve needs to be specified, which gives the non-dimensional thrust and torque fractions K_T, K_Q and the propeller efficiency η_0 as functions of the advance ratio J

$$J = \frac{v_A}{n \cdot D} \tag{6}$$

where v_A is the speed of advance of the propeller, n the rotation rate, and the D propeller diameter. Further inputs are the position of the propeller within the computational domain, the direction of the propeller rotational axis, and the direction of rotation, shown in Fig. 10.

Fig. 10 Position and diameter of Virtual Disc

For the simulations of self propelled model, the restrained model set up is used. The chosen propeller is B Wageningen 5 blades series. All parameters of propeller are reported in Table 6, together with K_T, K_Q and η_0 diagram given in Fig. 11.

Table 6 Propeller chosen for simulation of self propelled model

No. blades	5
A_E/A_0	0.85
P/D	0.95
D (m)	0.05
η_0	0.6289

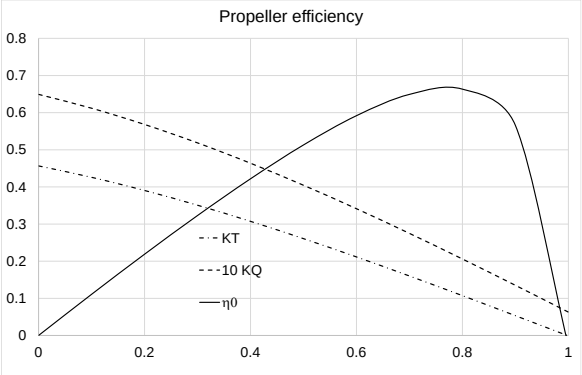

Fig. 11 Propeller characteristics - input data

Results of numerical self propulsion test are thrust force and wake coefficient. From thrust force the thrust deduction coefficient *1-t* is calculated and finally hull efficiency coefficient η_H. All results are given in Table 7 and in Fig. 12. Axial velocity field on virtual disc for model speeds 0.976, 1.301, 1.952 and 2.600 m/s is shown in Fig. 13, 14, 15 and 16, respectively.

Table 7 Results of self-propulsion numerical simulations

v_{model}	$R_{T\text{-}SWATH}$	T	*1-t*	*w*	*1-w*	η_H
(m/s)	(N)	(N)	-	-	-	-
0.976	2.8000	2.8036	0.9987	0.0570	0.9430	1.0591
1.301	3.1780	3.1818	0.9988	0.0171	0.9829	1.0162
1.952	5.9232	5.9302	0.9988	0.0077	0.9923	1.0066
2.603	9.6558	9.6676	0.9988	0.0047	0.9953	1.0035

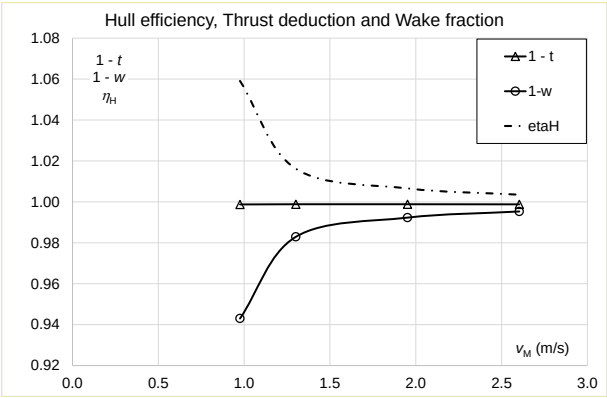

Fig. 12 Hull efficiency, Thrust deduction and Wake fraction coefficients

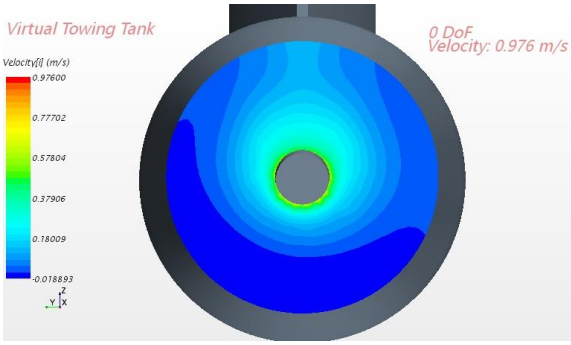

Fig. 13 Axial velocity field at v = 0.976 m/s

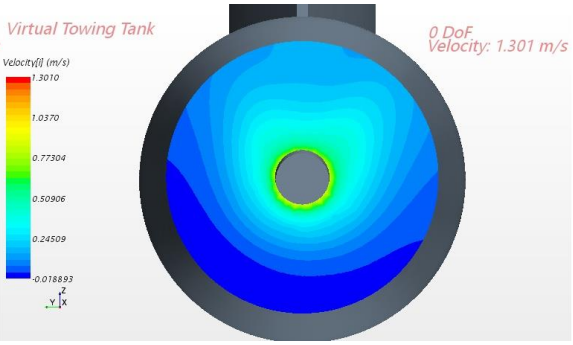

Fig. 14 Axial velocity field at v = 1.301 m/s

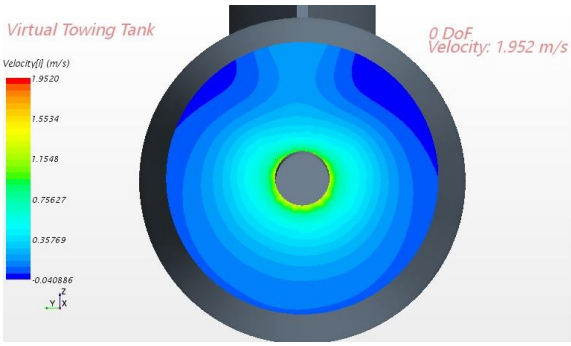

Fig. 15 Axial velocity field at v = 1.952 m/s

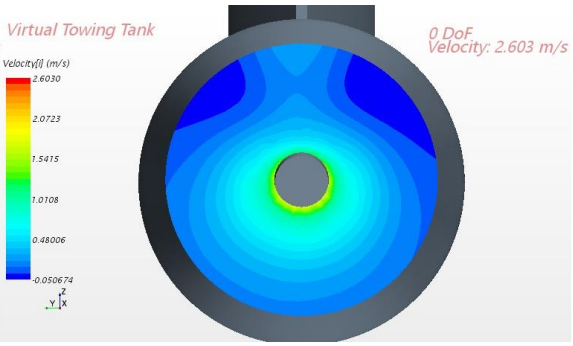

Fig. 16 Axial velocity field at v = 2.603 m/s

Kennell [17] reports SWATH thrust and wake coefficients experimental data and highlights the wake differences between monohull and SWATH. The major feature of SWATH wake is the strong wake deficit above the centerline of the propeller caused by the retarded flow due to the strut boundary layer. It was pointed out that the wake of SWATH at a particular propeller radius is uniform. Both conclusions have been observed and confirmed by performed CFD simulations. Furthermore, it can be seen that the SWATH hull efficiency coefficient η_H is close to 1, indicating considerably higher efficiency than monohull vessels, results obtained also by Kennell [17].

3.4 Grid Sensitivity Analysis

The grid sensitivity analysis has been performed for resistance test at model speed of 0.976 m/s for the simulation case 0 DOF, applying RANSE solver with exactly the same numerical model, discretization schemes and parameter settings on three different grids: Fine, Medium and Coarse. Starting from the coarse grid, the mesh size is progressively increased by a refinement ratio equal to $\sqrt{2}$ (called grid refinement index). The grid sizes and the computed model resistance are given in Table 8 and in Fig. 17.

Table 8 Change of Resistance results according to grid refinement

Grid	Mesh size	R_{SWATH}
	10^6	(N)
Coarse	0.9330	2.7782
Medium	1.3200	2.7544
Fine	1.8670	2.7356

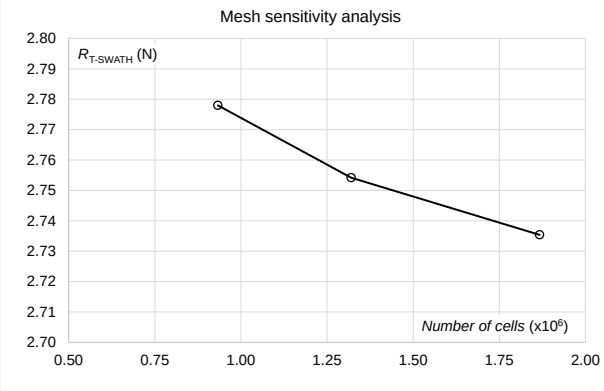

Fig. 17 SWATH total resistance variation for different mesh refinement

It can be observed from the Fig. 17, that $R_{T\text{-}SWATH}$ does not vary significantly with grid refinement and exhibits a sound convergence. The Medium grid has been used for the present work based on a trade-off between resolution and resource demand.

Uncertainty analysis has been performed according to ITTC 7.5-03-01-01 recommendations [18], using the method proposed by Tao and Stern [19]. Starting from the absolute differences among resistance values for Medium and Coarse meshes $\varepsilon_{M\text{-}C}$ and Fine and Medium meshes $\varepsilon_{F\text{-}M}$: 0.0238 and 0.0188 respectively, the calculation procedure is reported in Table 9.

Table 9 Uncertainty analysis assessment

$R_G = \frac{\varepsilon_{F-M}}{\varepsilon_{M-C}}$	$p_G = \frac{\ln \frac{\varepsilon_{F-M}}{\varepsilon_{M-C}}}{\ln \sqrt{2}}$	$P = \frac{p_G}{2}$	$\delta_G^* = \frac{\varepsilon_{F-M}}{\sqrt{2}^{p_G} - 1}$	$U_{GC} = 1.25 \cdot \lvert \delta_G^* \rvert$	$U_{GC}(\%) = 100 \cdot \frac{U_{GC}}{R_{T-Fine}}$
0.790	0.6805	0.34023	0.0072	0.009011	3.230

4. COMPARISON WITH EXPERIMENTAL DATA

CFD analysis reported in this paper follows the experimental campaign concerning SWATH configurations performed at Hydrodynamic Lab of University of Naples Federico II. CFD simulations are compared with the results of the calm water tests performed on this scale model and already presented in [10].

4.1 Resistance set up

Resistance set up for SWATH model is shown in Fig. 18. The towing line has been connected to a load cell HBM with maximum load of 5 kg. The towing line height was the lowest possible that means at waterline with the smallest possible angle to keep the towing line out of the water. Due to the very small value of model resistance, even at the lowest possible acceleration of the towing carriage, the model, free to surge, tended to oscillate longitudinally. Therefore all tests are performed with a counter pull force, (on the left in Figure 18) connected to the model, fixed at the same point of the towing line with opposite direction. A 500 g counter pull made motion steady.

Resistance tests have been performed with trim restrain acting soon after trim angles are recorded. This in order to appreciate the maximum possible free ride speed and then to evaluate the required action of trim correctors. Experimental setup is very close to restrained model numerical simulation set up.

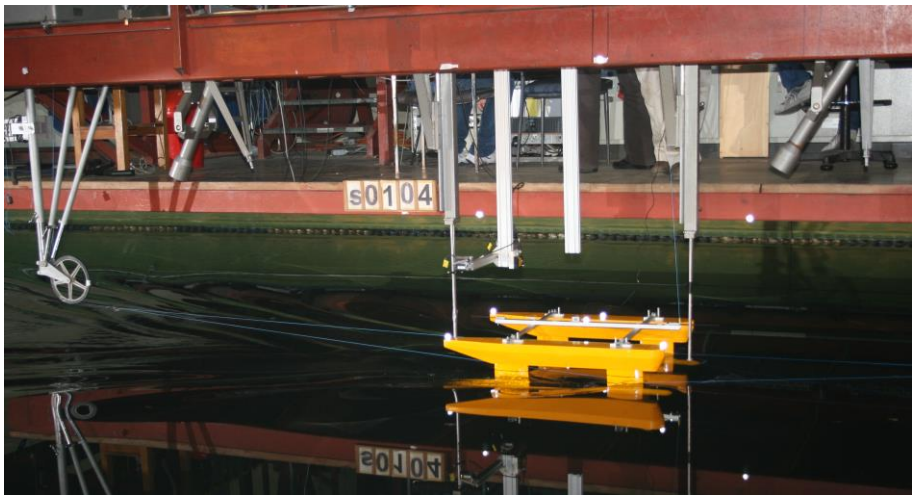

Fig. 18 Resistance and seakeeping set up

The turbulence of the flow around torpedos has not been stimulated, as the Reynolds number *Re* value was over $9*10^5$ at the lowest tested speed. The struts at lowest speed values present lower *Re*, but the presence of torpedo heads has been considered an adequate factor for turbulence flow stimulation. The resistance tests are performed for eight model speeds. Tested velocities, measured resistance and measured standard deviations are reported in Table 10, where the values in bold announce the direct comparison with CFD simulation.

The ITTC Seakeeping Committee (2011) in recommended procedures 7.5 adopted ISO-GUM approach to conducting uncertainty analysis of experimental results. The ISO-GUM recognizes two groups of uncertainties, type A and type B based on way in which the uncertainty is evaluated. Type A represents the random category of uncertainty evaluated by using statistical analysis of repeated measurements of the same observation. The results reported in Table 10 are obtained as mean value multiplied bias of load cell (1/1000 N). Type B uncertainty can be estimated from quoted values of uncertainty, assuming statistical distribution of the parameters and factors depending on a level of confidence in the measurement. Generally, type B uncertainty is considered as normally distributed around some mean and for 95% level of confidence, factor 1.96 has to be applied to the standard deviations. Finally it can be seen that total uncertainty *u*, except for the speed 0.651 m/s, is ranging from 3 to 4 % and about the same as the numerical ones.

Table 10 Comparison of experimental and numerical results for SWATH model resistance

V	σ_V	Fr_T	R_T	σ_{R_T}	*Type A*	*Type B*	*u*	*u (%)*
(m/s)	**(m/s)**	-	**(N)**	**(N)**	**(N)**	**(N)**	**(N)**	**(N)**
0.976	**0.002**	**0.316**	**2.609**	**0.059**	0.00261	0.115	0.115	4.42
1.301	**0.002**	**0.422**	**2.883**	**0.059**	0.00288	0.115	0.115	4.00
1.627	0.002	0.528	4.276	0.059	0.00428	0.115	0.115	2.70
1.952	**0.002**	**0.633**	**5.943**	**0.088**	0.00594	0.173	0.173	2.91
2.277	0.002	0.738	7.992	0.157	0.00799	0.308	0.308	3.85
2.603	**0.003**	**0.844**	**10.091**	**0.177**	0.01009	0.346	0.346	3.43

The measured total resistance was further subdivided into frictional and residual components according to ITTC 57 procedure. Within standard ITTC correlation procedure the measured resistances are reported in nondimensional form through "geosim" coefficients defined as

$$C_T = \frac{R_T}{0.5 \cdot \rho \cdot v^2 \cdot WS}$$

where

v – model velocity, m/s

WS – model wet surface, m^2

ρ – water density, kg/m^3

ITTC-57 correlation procedure defines frictional coefficient of a corresponding plate C_{F0} as

$$C_{F0} = \frac{0.075}{(\log Re - 2)^2}$$

Re – Reynolds number defined as $Re = \frac{v \cdot L}{\upsilon}$

υ - kinematic viscosity, m^2/s

Due to the different strut and torpedo lengths, their Rn and C_{F0} will be different and therefore the resistance breakdown is done as follows:

$$R_{F-4STRUT} = 4 \cdot (0.5 \cdot \rho \cdot g \cdot C_{F0-STRUT} \cdot WS_{STRUT})$$

$$R_{F-2TORPEDO} = 2 \cdot (0.5 \cdot \rho \cdot g \cdot C_{F0-TORPEDOT} \cdot WS_{TORPEDO})$$

$$R_{R-SWATH} = R_{T-SWATH} - R_{F-2TORPEDO} - R_{F-2STRUT}$$

$$C_{R-SWATH} = \frac{R_{R-SWATH}}{0.5 \cdot \rho \cdot v^2 \cdot (2 \cdot WS_{TORPEDO} + 4 \cdot WS_{STRUT})}$$

For the calculation of residual coefficient shown in Fig. 19, the static wetted surface and ITTC 57 correlation procedure have been used. Results shown in Fig. 19 confirm main findings reported before on the necessity of stabilisation device after, in this case, Fr_T 0.422. The difference between C_R and C_W curves at lower speeds is only due to "form factor", or more correctly, due to the intrinsic difference in the consideration of frictional resistance component by CFD simulation and experimental results based on ITTC 57 frictional line. Beside that the variation of dynamic wetted surface should be taken into account to get fair analysis of experimental resistance components. Nevertheless the obtained results for resistance coefficients can be considered very promising and future experimental campaign will be aimed at form factor and dynamic wetted surface determination.

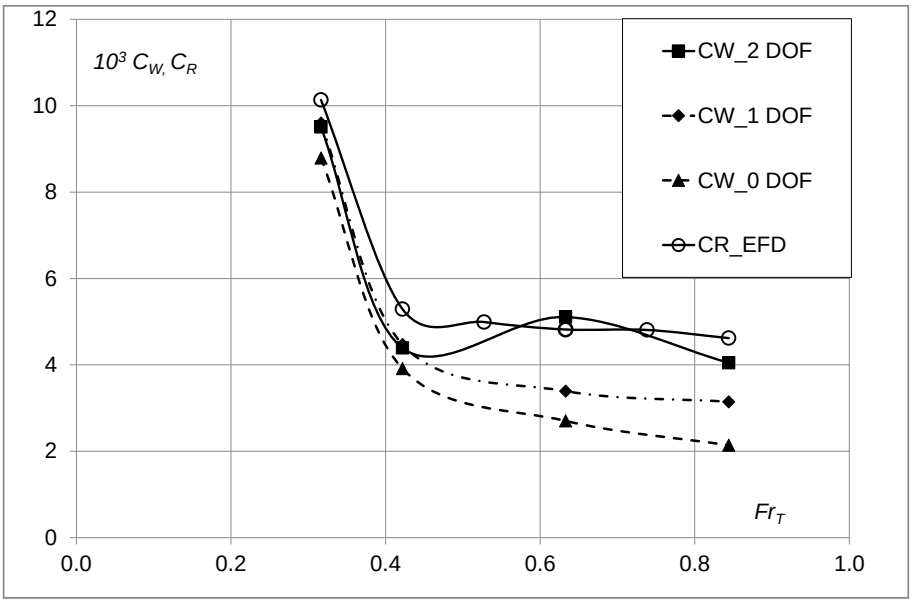

Fig. 19 Comparison of CFD and EFD resistance coefficients

5. CONCLUSIONS

Aim of this paper is to report the introduction of numerical simulation within a research program focused on small size SWATH vessels and to identify the reliability and potential of CFD analysis within design and development of SWATH hull forms.

The reported results concern calm water resistance analysis and hull efficiency coefficients. They are both of main importance in the preliminary design procedure for a sound assessment of powering performances. The comparison with experimental data reported in this paper allows to consider CFD as a reliable tool for the assessment of further developed similar hull forms.

The numerical investigation identifies the maximum possible free ride speed value without longitudinal instability. CFD results at higher speeds allow to identify and to assess input data for trim correctors and stabilizing fins.

The confirmation of expected very high hull efficiency allows reliable shaft horsepower prediction and highlights one of the peculiar favourable SWATH characteristics.

The further development of this research concerns the improvement of critical aspects in experimental resistance assessment as well as the study on effect of torpedo's immersion on suction effect both numerically and experimentally; the numerical simulation of rough water SWATH behaviour and the comparison of seakeeping assessments in head and following seas.

ACKNOWLEDGMENTS

This work has been supported by Sommella & Contardi MARINE S.r.l within research commitment to Department of Industrial Engineering, University of Naples Federico II. The Authors are grateful to Mr. Edoardo Contardi and Mr. Carmine Sommella for their encouragements and collaboration. The Authors gratefully acknowledge the availability of 32 processors at Calculation Centre SCoPE, University of Naples, and thanks SCoPE academic staff for the given support.

NOMENCLATURE

B – maximum breadth (m)

CG – centre of gravity (m)

D – propeller diameter (m)

D_T – torpedo diameter (m)

D_T/T – ratio between torpedo diameter and SWATH draft

Fr– Froude number based on ship length, $Fr = \frac{v}{\sqrt{g \cdot L}}$

Fr_T – Froude number based on torpedo's length

J – advance ratio $J = \frac{v_A}{n \cdot D}$

K_Q – non-dimensional torque $K_Q = \frac{Q}{\rho \cdot n^2 \cdot D^5}$

K_T – non-dimensional thrust $K_T = \frac{T}{\rho \cdot n^2 \cdot D^4}$

LCG – longitudinal position of centre of the gravity (m)

L_{OA} – length over all (m)

L_S – strut length (m)

L_T – torpedo length (m)

n – propeller rotation rate

Q – torque (Nm)

Re – Reynolds number $Re = \frac{v \cdot L}{\upsilon}$

$R_{F\text{-}SWATH}$– frictional resistance in calm sea condition (N)

$R_{T\text{-}SWATH}$– total resistance in calm sea condition (N)

T –thrust (N)

t – thrust coefficient

v – ship, model speed (m/s)

w – wake coefficient

Δ – displacement (N)

λ- ship – model scale ratio

η_0 – propeller efficiency

η_H – hull efficiency

REFERENCES

[1] Lee C.M., Curphey M.: Prediction of motion, stability and wave load of Small Waterplane Area Twin Hull Ships, SNAME Transactions, 85, pp. 94-130, 1977.

[2] Salvesen, N., von Kerczek, C.H., Scragg, C.A., Cressy, C.P., Meihold, M.J.: Hydro-Numeric Design of SWATH Ships, *SNAME Transactions*, Vol. 93, pp. 325-346, 1985.

[3] Papanikolaou A., Androulakakos M.: Hydrodynamic Optimization oh High-Speed SWATH, FAST 91, pp. 507-522, 1991.

[4] Schellin T.E., Papanikolaou A.: Prediction of Seakeeping Performance of a SWATH Ship and Comparison with Measurements, FAST 91, pp. 811-827, 1991.

[5] Beena V.I., Subramanian V.A.: Parametric studies on seaworthiness of SWATH ships, Ocean Engineering 30 (2003) 1077–1106, 2003.

[6] Yoshida M., Kihara H., Iwashita H., Kinoshita T.: Seaworthiness of Resonance-Free SWATH with Movable Fins as an Oceangoing Fast Ship, *11th International Conference on Fast Sea Transportation FAST 2011*, Honolulu, Hawaii, USA, 2011.

[7] Brizzolara S., Chryssostomidis C.: Design of an Unconventional ASV for Underwater Vehicles Recovery: Simulation of the motions for operations in rough sea, *ASNE Int. Conference on Launch & Recovery*, Nov. – 14-15, 2012.

[8] Brizzolara S., Bovio M., Federici A., Vernengo G.: Hydrodynamic Design of a Family of Hybrid SWATH Unmanned Surface Vehicles, 11th International Conference on Fast Sea Transportation FAST 2011, Honolulu, Hawaii, USA, 2011.

[9] Qian P.,Yi H., Li Y.: Numerical and experimental studies on hydrodynamic performance of a small-waterplane-area-twin-hull(SWATH) vehicle with inclined struts, Ocean Engineering 96 (2015), 181-191, 2015.

[10] Begovic E., Bertorelo C.: Small Waterplane Area Twin Hull for maxi and mega-yacht design, International Conference on the Design and Construction of Super & Mega Yachts, Genova, 13-14 May, (2015), RINA, UK, pp. 53-64, 2015.

[11] Renilson M.R.: Submarine Hydrodynamics, *Springer*, 2015.

[12] Renilson M. R., Polis C., Ranmuthugala D., Duffy J.: Prediction Of The Hydroplane Angles Required Due To High Speed Submarine Operations Near The Surface, Warship 2014: Naval Submarines & UUV's, 18-19 June 2014, Bath, UK, RINA, 2014.

[13] Renilson, M.R. and Ranmuthugala, D., The effect of proximity to free surface on the optimum length/diameter ratio for a submarine, 1st Int. Conference on Submarine Technology and Marine Robotics (ICSTaMR 2012), 13 – 14 Jan. 2012.

[14] Bhattacharyya R.: Dynamics of Marine Vehicles, *John Wiley & Sons Inc*, 1978.

[15] Visonneau, M., Queutey, P., Deng, G.B.: EFFORT Work Package 4- ECN-CNRS Report, Internal report for EU project: G3RD-CT-2002-00810-European Full Scale Flow, 2005.

[16] Bugalski T.: Study on Numerical Prediction of Effective Wake Field, proceedings of Numerical Towing Tank Symposium NUTTS 2011, Southampton, UK, 2011.

[17] Kennell C.: SWATH Ships, Technical Research Bulletin No7-5, SNAME, 1992.

[18] ITTC Recommended Procedures and Guidelines - 7.5-03 -01-01: Uncertainty Analysis in CFD Verification and Validation Methodology and Procedures, 2008.

[19] Tao, X. and Stern F.: Factors of Safety for Richardson Extrapolation, Journal of Fluids Engineering, Vol. 132, 061403-1, 2010.

[20] CD-Adapco: Star CCM+ v. 9.06 User's Manual, 2014.

Submitted: 06/07/2015

Accepted: 22.09.2015.

Ermina Begovic, begovic@unina.it
Carlo Bertorello
Simone Mancini
University of Naples Federico II
Department of Industrial Engineering
Via Claudio 21, 80125 Naples, Italy